Microscopic Coexistence of Superconductivity and Antiferromagnetism in Underdoped $Ba(Fe_{1-x}Ru_x)_2As_2$

Long Ma,[1] G. F. Ji,[1] Jia Dai,[1] X. R. Lu,[1] M. J. Eom,[2] J. S. Kim,[2] B. Normand,[1] and Weiqiang Yu[1,*]

[1]*Department of Physics, Renmin University of China, Beijing 100872, China*

[2]*Department of Physics, Pohang University of Science and Technology, Pohang 790-784, Korea*

(Received 15 May 2012; published 7 November 2012)

We use ^{75}As nuclear magnetic resonance to investigate the local electronic properties of $Ba(Fe_{1-x}Ru_x)_2As_2$ ($x = 0.23$). We find two phase transitions: to antiferromagnetism at $T_N \approx 60$ K and to superconductivity at $T_C \approx 15$ K. Below T_N, our data show that the system is fully magnetic, with a commensurate antiferromagnetic structure and a moment of $0.4\mu_B$/Fe. The spin-lattice relaxation rate $1/^{75}T_1$ is large in the magnetic state, indicating a high density of itinerant electrons induced by Ru doping. On cooling below T_C, $1/^{75}T_1$ on the magnetic sites falls sharply, providing unambiguous evidence for the microscopic coexistence of antiferromagnetism and superconductivity.

DOI: 10.1103/PhysRevLett.109.197002 PACS numbers: 74.70.−b, 76.60.−k

In the iron-based superconductors, superconductivity (SC) is achieved on suppressing a long-ranged antiferromagnetic order [1] by doping or pressure. At this phase boundary, much attention has been drawn to the question of whether SC may coexist with antiferromagnetism (AFM). Proposals for possible coexisting phases have included commensurate [2] and incommensurate [3–5] magnetic structures, competition between AFM and SC [2,4–7], and variations in the size of the ordered moment [8,9] or the pairing symmetry [10,11]. No consensus has yet been reached on the pairing mechanism or the possible phenomena arising from the interplay of AFM and SC. For most materials, local probe studies on high quality samples are required as a matter of urgency to distinguish the key properties of microscopic coexistence from any form of phase separation.

Because Ru is a 4*d* counterpart of Fe, it is expected to be an isovalent substituent. Isovalent substitution of P for As has been used to investigate the transition between [12], and the possible coexistence of Ref. [7], AFM and SC in $BaFe_2(As_{1-x}P_x)_2$ powders. The suppression of AFM by doping appears to be rather slow also in $Ba(Fe_{1-x}Ru_x)_2As_2$, and both transport [13] and angle-resolved photoemission studies [14–16] indicate that changes in the band structure with Ru doping are small. Crucially, some signs of coexistence between AFM and SC have been observed by bulk probes [17,18] in the underdoped region $0.15 \leq x \leq 0.3$. This slow suppression of AFM and the broad regime of coexistence offer a valuable opportunity to seek out and characterize a microscopic coexistence with minimal effects from doping inhomogeneity.

In this Letter, we use ^{75}As nuclear magnetic resonance (NMR) as a local probe to investigate Ru doping effects and the microscopic coexistence of AFM and SC in single crystals of $Ba(Fe_{0.77}Ru_{0.23})_2As_2$. This underdoped system has several properties quite distinct from the parent compound $BaFe_2As_2$. Although the doping produces no strong changes in carrier density and magnetic correlations above T_N, below this the ^{75}As spectrum shows fully magnetic signals and the AFM structure is commensurate, with a large moment of approximately $0.4\mu_B$/Fe. Below T_C, the spin-lattice relaxation rate $1/^{75}T_1$ shows a superconducting gap opening on the magnetic sites, providing incontrovertible local evidence for the microscopic coexistence of AFM and SC. We observe a high density of itinerant electrons below T_N, which constitutes clear experimental evidence for the effect of Ru doping in the magnetic state and offers an important clue to understanding the interplay of SC and magnetic order in Fe-based superconductors.

We begin by considering the nature of the evidence for coexistence. Much of the discussion in pnictides concerns nonisovalent doping of $BaFe_2As_2$, particularly $Ba(Fe_{1-x}Co_x)_2As_2$ [19], where the reported coexistence occurs over a very narrow range of doping. In most experiments, the evidence is indirect, in that muon spin resonance is used to probe magnetic order but bulk measurements are used for the superconductivity; NMR studies showing bulk superconductivity on the magnetic sites, with no mixing of paramagnetic contributions, are still lacking [4,20]. The situation is complicated by the question of sample homogeneity [2,9,20], an extreme example of which has emerged recently in the "microscopic phase separation" of alkali-intercalated FeSe [21]. Here we provide direct and unambiguous evidence for the coexistence of AFM and SC by using NMR, a local probe sensitive to both types of order on the atomic scale. In the process we will eliminate any sample inhomogeneity-induced phase separation of AFM and SC regions, and also any type of concomitant proximity-effect SC in AFM regions.

Returning to our target material, $Ba(Fe_{1-x}Ru_x)_2As_2$, the isovalent suppression of AFM by Ru doping is so far not well understood. Theoretically, it has been proposed that the more extended *d* orbitals on the Ru sites should weaken AFM order [22]. Experimental investigation is required to address whether this weakening is caused by a chemical

 © 2012 American Physical Society

pressure [13], a magnetic dilution [15], an effective doping, or a combination of effects, and the properties of the phases may vary strongly under the different scenarios. As one example, a nodal superconductivity has been suggested in underdoped $Ba(Fe_{1-x}Ru_x)_2As_2$ [23], and controversy remains over its possible origin in the reduced c-axis lattice parameter [23], in a magnetic effect [11], or in some other coexistence phenomenon.

Our $Ba(Fe_{0.77}Ru_{0.23})_2As_2$ single crystals were synthesized by the flux-grown method with FeAs as flux [18]. We stress here and below that bulk (near 100%) superconductivity has been reported in crystals grown in the same batch as ours, on the basis of thermal conductivity measurements [23]. The chemical composition was determined by energy-dispersive x-ray measurements. For our NMR experiments, single crystals with dimensions of approximately $3 \times 1.5 \times 0.1$ mm^3 were chosen. The NMR measurements were performed on ^{75}As nuclei ($S = 3/2$) under a magnetic field of 10 T and in two different field orientations, using a TecMag spectrometer. The frequency-swept NMR spectra were obtained by integrating the Fourier transform of the spin-echo intensity. The spin-lattice relaxation rate $1/^{75}T_1$ is measured with the inversion-recovery method, by fitting the magnetization to the functional form $I(t)/I(0) = 1 - a(0.1e^{-t/T_1} + 0.9e^{-6t/T_1})$.

Our $Ba(Fe_{0.77}Ru_{0.23})_2As_2$ sample is clearly underdoped, as shown by the presence of two separate transitions in the resistivity and the susceptibility, presented respectively in Figs. 1(a) and 1(b). The in-plane resistivity $\rho(T)$ decreases almost linearly with temperature from 300 K down to 60 K. The low-temperature upturn in $\rho(T)$ indicates the simultaneous structural and AFM transition at $T_N \approx 60$ K [17,18], and the sharp drop of $\rho(T)$ to zero is the superconducting transition at $T_C \approx 15$ K. A schematic phase diagram for $Ba(Fe_{1-x}Ru_x)_2As_2$, based on the data of Ref. [17], is shown in the inset of Fig. 1(a); the squares are our own data (not shown) for samples of different dopings, and the sample used for our NMR experiments is clearly in the underdoped regime. The dc susceptibility shows full demagnetization just below T_C in Fig. 1(b). Bulk superconductivity under the 10 T NMR field is also monitored *in situ* by the resonance frequency of the NMR circuit, as shown in the inset of Fig. 1(b). The rapid increase in frequency below T_c, which is reduced to 12 K at 10 T, represents a decrease in the ac susceptibility due to superconductivity.

The ^{75}As spectra for a range of temperatures are shown in both field orientations in Figs. 2(a) and 2(b). For $H \parallel c$, the FWHM height of the central transition is approximately 40 kHz at $T = 80$ K. The spectrum broadens significantly and splits into two separate peaks on cooling below $T_N = 60$ K, as expected at the AFM transition. For $H \parallel ab$, the FWHM is 42 kHz at $T = 80$ K, and also broadens below T_N, the single peak shifting to a slightly higher frequency.

The spectral splitting we observe below T_N for $H \parallel c$ and the frequency shift for $H \parallel ab$ both demonstrate that our crystal is fully magnetic, with a commensurate A-type

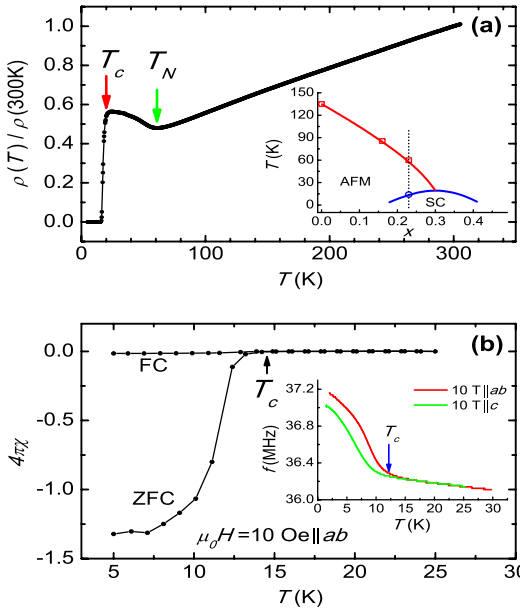

FIG. 1 (color online). (a) In-plane resistivity of the $Ba(Fe_{0.77}Ru_{0.23})_2As_2$ crystal on cooling at zero field. Inset: Schematic phase diagram of $Ba(Fe_{1-x}Ru_x)_2As_2$, where the dotted line represents the doping of our crystals. (b) dc susceptibility during field cooling (FC, with a 10 Oe field applied in the crystalline ab plane) and zero-field cooling (ZFC). Inset: Resonance frequency of the NMR circuit as a function of temperature, with a 10 T field applied in two orientations.

(striped) AFM order. Located above the centers of the Fe squares, the ^{75}As nuclei detect an off-diagonal contribution from Fe moments in the stripe configuration, and the internal static hyperfine field is oriented along the c axis [24]. The ^{75}As spectrum below T_N is therefore split, with two peak frequencies $f = \gamma H_{\text{total}} = \gamma(H_{\text{ext}} \pm H_{\text{in}})$, for $H \parallel c$, whereas for $H \parallel ab$ there is a spectral shift with one peak frequency $f = \gamma H_{\text{total}} = \gamma\sqrt{H_{\text{ext}}^2 + H_{\text{in}}^2}$; H_{ext} and H_{in} refer respectively to the applied field and the internal

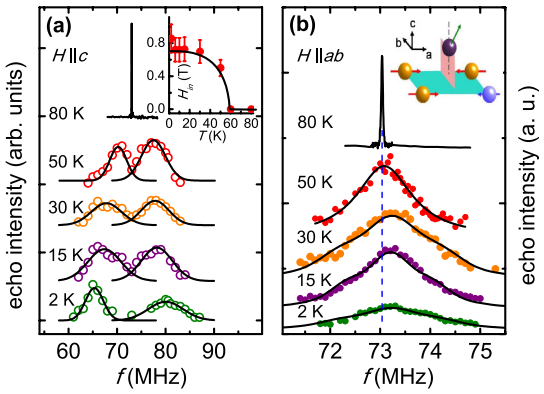

FIG. 2 (color online). ^{75}As NMR spectra with a 10 T magnetic field applied (a) along the c axis and (b) in the ab plane of our single crystal. Inset of (a): Static hyperfine field at ^{75}As sites as a function of temperature. Inset of (b): Representation of one magnetic configuration in the presence of Ru dopants and the resulting ^{75}As hyperfine field.

hyperfine field. For $H \parallel c$, the spectral weight at the paramagnetic resonance frequency decreases rapidly below T_N, essentially vanishing below 30 K [Fig. 2(a)]. This observation means that every ion in the sample is magnetic. It also excludes incommensurate magnetism, as suggested [25] in NaFeAs, which would also require a much higher spectral weight at this frequency. Similarly for $H \parallel ab$, the spectrum at this frequency [dashed line in Fig. 2(b)] contains no detectable residual peak below T_N.

We estimate the internal field $H_{\rm in}$ from the shift in peak frequencies. As shown in the inset of Fig. 2(a), $H_{\rm in}$ increases with decreasing temperature, reaching $H_{\rm in} = 0.7$ T at $T = 2$ K. Under the assumption that the off-diagonal hyperfine coupling is the same as in $BaFe_2As_2$, $A_{\rm hf}^{\rm ac} = 0.43$ T$/\mu_B$ [24], we estimate the magnetic moment as $H_{\rm in}/4A_{\rm hf}^{\rm ac} \approx 0.4\mu_B$/Fe at $T = 2$ K, consistent with the neutron scattering result at a similar doping [17]. Further, the large line width for $H \parallel ab$ can be fully explained as a Ru doping effect: with one Ru atom in a square unit [inset of Fig. 2(b)], the ^{75}As nuclei pick up both ab plane and c axis field components due to the unbalanced hyperfine fields from the Ru and Fe moments. The solid lines in Fig. 2 were drawn by taking the statistical distribution of square units corresponding to 23% Ru doping and applying a Gaussian broadening. If we assume further that ^{75}As has the same hyperfine coupling to Ru as to Fe, we may estimate a lower bound for the hyperfine field as $0.25\mu_B$/Ru at $T = 2$ K. This result once again supports a fully magnetic state, but with a magnetic dilution effect on the Ru sites.

At this point we discuss in detail the question of doping inhomogeneity. This is a crucial issue in Fe superconductors, where the unexpected electronic properties of non-stoichiometric materials turn out in several cases to be due to inclusions of phases which differ in chemical composition. The most extreme example is alkali-intercalated FeSe, where the AFM and SC phases show a microscale phase separation [21], and this is clearly a possibility we must eliminate in $Ba(Fe_{1-x}Ru_x)_2As_2$. In our data (Fig. 2), the $H \parallel c$ spectrum at 15 K shows some small but complicated features beyond the statistical fit, which are probably caused by minor doping inhomogeneities; related strain or disorder effects are to be expected at this near-critical doping, where we believe the system is close to the transition to zero magnetic order. Above T_N, we find no decrease in spectral weight in the paramagnetic frequency range between 60 and 120 K (data not shown), which indicates that the impact of inhomogeneity on the magnetism is weak. In general, we expect that the local Ru doping is related directly to the on-site moment, and hence to the width of the NMR lines below T_N. From our spectral-weight analysis, we estimate that the fraction of sites in a paramagnetic phase (zero internal field) is below 0.05%, while for those with moments 0.7–0.8μ_B/Fe (close to the undoped value) it is approximately 3%. We stress that our data (Fig. 2) show no evidence for bimodal distributions, or any other clustering suggesting a favored doping value away from the average, which would be an essential sign of phase separation. We remind the reader that microscopic and bulk phase separation are essentially the same to a probe as local as NMR. We define microscopic coexistence as the statement that the majority of the sample hosts both SC and AFM order. It is therefore not excluded if small fractions at extreme doping inhomogeneities lack one type of order or the other.

The fact that our NMR signals are fully magnetic below T_N is already an indication for the coexistence of AFM and SC, but we defer a full discussion until our presentation of the spin dynamics (below). The Knight shift, $^{75}K(T)$, and spin-lattice relaxation rate, $1/^{75}T_1(T)$, at the peak frequency are shown in Figs. 3(a) and 3(b) for the two field orientations. We have also measured the same quantities for $BaFe_2As_2$ single crystals, and show the data in Fig. 3 for comparison.

Above T_N, spin fluctuation effects are evident in both ^{75}K and $1/^{75}T_1$. By fitting the relaxation rate to a sum of Curie-Weiss and Korringa components, $1/^{75}T_1 = AT/(T-\theta) + BT$, we find that $1/^{75}T_1$ in the doped sample has a strong Curie-Weiss contribution with $\theta \approx 46$ K for $H \parallel ab$ [shown as the solid line in Fig. 4(a)]. Such a form is consistent with low-energy AFM spin fluctuations in itinerant systems [26], and the diverging behavior of $1/^{75}T_1$ at $T = T_N$ indicates the magnetic transition. $^{75}K(T)$ measures the spin susceptibility at $q = 0$ and therefore shows no low-energy AFM spin fluctuations, but its weakly quadratic temperature dependence on top of a constant contribution from itinerant electrons is fully consistent with local-moment fluctuations [27]. Comparison with $BaFe_2As_2$ shows that Ru doping causes no strong changes in ^{75}K or $1/^{75}T_1$ above T_N, as also reported in Ref. [28]. Because these quantities measure magnetic correlation effects and the electronic density of states on the Fermi surface, this weak dependence is consistent with a nearly isovalent doping effect [14,15,22].

The superconducting transition is clearly visible in the spin-lattice relaxation rate. In Fig. 4(a) we show

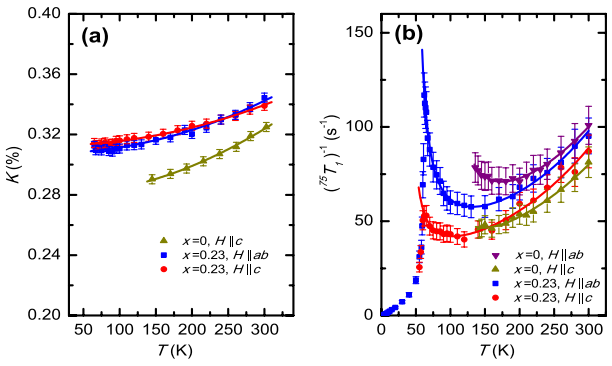

FIG. 3 (color online). (a) $^{75}K(T)$ as a function of temperature for $Ba(Fe_{1-x}Ru_x)_2As_2$ ($x = 0$, 0.23) with two field orientations. The solid lines are a fit to the function $^{75}K(T) = a + bT^2$. (b) $1/^{75}T_1$ as a function of temperature with two field orientations. For each doping, the solid line above T_N is a fit to $1/^{75}T_1 = AT/(T-\theta) + BT$.

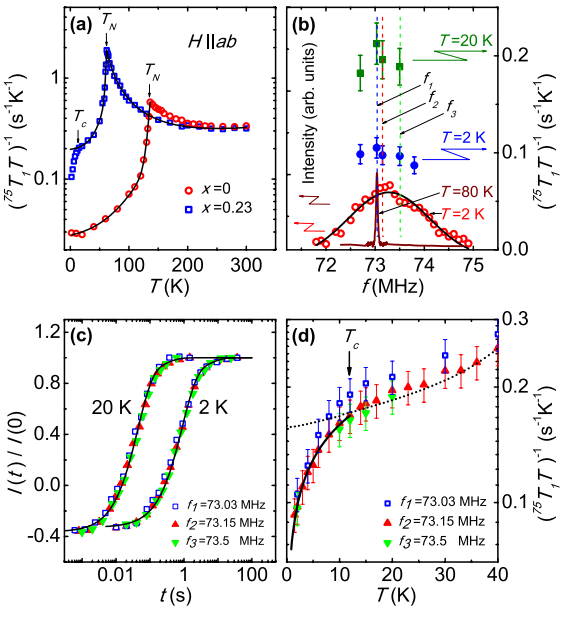

FIG. 4 (color online). (a) $1/^{75}T_1T(T)$ on semilog axes for $Ba(Fe_{1-x}Ru_x)_2As_2$ ($x = 0$, 0.23). Solid lines below T_N indicate the trend towards a low-temperature constant. (b) ^{75}As spectrum at $T = 2$ and 80 K, shown with $1/^{75}T_1T$ at $T = 20$ and 2 K. (c) ^{75}As magnetization recovery curve at three frequencies. The solid line represents a fit using a single T_1 component. (d) $1/^{75}T_1T$ at low temperatures for the three frequencies f_1, f_2, and f_3 (see text).

$1/^{75}T_1T(T)$ with $H \| ab$ for comparison with Fermi-liquid behavior ($1/T_1T$ constant). On cooling below 12 K, the spectral weight of the NMR signal is reduced (data not shown) and $1/^{75}T_1T$ drops abruptly; both observations are signatures of superconductivity fully consistent with the ac susceptibility data. We have also measured $1/^{75}T_1$ across the spectrum at $T = 2$ and 20 K, shown as a function of frequency in Fig. 4(b). The reduced, uniform value of $1/^{75}T_1T$ at 2 K supports the opening of a uniform superconducting gap below T_C. We further measured $1/^{75}T_1(T)$ at selected frequencies f_1, f_2, and f_3, taken close to the peak frequency as shown in Fig. 4(b). Signals at f_2 and f_3 are clearly due to magnetic sites, as their echo intensity is zero above T_N. Uniform superconductivity is clearly present over a frequency range with at least 70% of the spectral weight, for sites with magnetic moments centered at $0.4\mu_B$. Figure 4(c) demonstrates that the ^{75}As magnetization is fitted very well by a single T_1 component at all of the selected frequencies, excluding any phase separation. In Fig. 4(d), $1/^{75}T_1T$ is shown at the same three frequencies; the fact that all drop identically at T_c suggests that superconductivity in our sample is very homogeneous.

The abrupt drop in $1/^{75}T_1T$ is unambiguous, local evidence for the superconducting gap opening on the magnetic sites. The results detailed in the previous paragraph, namely the uniform nature of our $1/T_1$ data and the absence of bulk paramagnetism, supplemented by the thermal conductivity results of Ref. [23], indicate that this superconductivity is a homogeneous, bulk phenomenon and that it cannot be a proximity effect arising from nonmagnetic regions. Our results therefore cannot be interpreted as a bulk or microscopic phase separation, and establish clearly a microscopic coexistence of SC and AFM in $Ba(Fe_{0.77}Ru_{0.23})_2As_2$.

To further understand the Ru doping effect, one may compare $1/^{75}T_1$ below T_N for $Ba(Fe_{0.77}Ru_{0.23})_2As_2$ and $BaFe_2As_2$. This quantity tends to level off to a constant value [Fig. 4(a)], as expected for a suppression of magnetic fluctuations far below T_N. However, the constant value is 1 order of magnitude higher for the doped sample. Because $1/^{75}T_1T$ is a measure of the electron density of states on the Fermi surface when spin fluctuations are weak, our data show that the density of itinerant electrons below T_N is increased by a factor of 3–4 due to Ru doping. To our knowledge, this clear experimental evidence for doping-induced itinerant electrons, going beyond a simple isovalent effect, has not been obtained before. These itinerant electrons have significant implications for both the AFM and the SC phases.

Considering first the AFM phase, the doping-induced itinerant electrons may be connected with magnetic dilution. The weakening of antiferromagnetic correlations upon Ru doping suggests that the itinerant electrons are either nonmagnetic or weakly magnetic. The magnetism of the parent compound is believed to have a local-moment origin in the valence electrons. Because Ru has more extended d orbitals than Fe, the presence of itinerant electrons can be understood by shifts of magnetic valence electrons to the Fermi surface. Thus our results provide experimental support for the proposed magnetic dilution effect [14–16] in a band picture. We stress, however, that magnetic dilution may be an effect rather than a cause of electron redistribution, and chemical pressure is thought to have a key role in Ru doping [22].

Turning next to the SC phase, the itinerant electrons we observe may be the key to a full understanding of superconductivity in the magnetic state. We note that a temperature decrease from T_C down to 2 K causes $1/^{75}T_1T$ to fall by a factor of 2 [Fig. 4(a)], which suggests that it is the itinerant electrons that condense into superconducting pairs. It is highly compelling to propose that these itinerant electrons are required for the phase coherence of superconductivity, and that a high density of nonmagnetic or weakly magnetic electrons may be a prerequisite for the coexistence of AFM and SC. Our results therefore serve as valuable new input for microscopic models of coexistence.

We stress that we do not observe an appreciable drop of the AFM moment below T_C [inset of Fig. 2(a)]; i.e., we find little evidence of competition between the two types of order, in contradiction to some theories [2,10]. Our data suggest rather that the itinerant electrons are nonmagnetic, and occupy different parts of the Fermi surface from the magnetic electrons. Quantitatively, the ordered moment at this doping ($0.4\mu_B$/Fe) may be too large to be affected appreciably by SC, whereas materials with slightly higher doping (lower moment) may show some suppression of AFM by SC.

We close by commenting on the pairing symmetry. The coexistence of AFM and SC is consistent [10] with the $s_{\pm}$ superconducting order parameter proposed in other pnictides [29–36]. Our results [Fig. 4(d)] show that $1/^{75}T_1T$ is rather large at 2 K, even when the relatively high magnetic field is considered; this suggests a high density of low-energy excitations in the SC state, which is consistent with recent suggestions of nodal superconductivity in underdoped $Ba(Fe_{1-x}Ru_x)_2As_2$ [23]. "Accidental" line nodes occurring due to the band dispersion in k_z have been proposed in the $BaFe_2(As_{0.7}P_{0.3})_2$ [37]. Alternatively, the coexistence of long-range AFM with SC may in fact cause a nodal gap [11]. Although we cannot distinguish whether our samples fit one or both scenarios, our observation of coexisting AFM and SC offers essential input for understanding the excitation spectrum in underdoped Fe superconductors.

In summary, we have used ^{75}As NMR to study high-quality single crystals of $Ba(Fe_{0.77}Ru_{0.23})_2As_2$. The NMR spectra below T_N show that the sample is fully magnetic, and are consistent with commensurate antiferromagnetism in which the magnetic moments are reduced by comparison with $BaFe_2As_2$. We find a sharp drop in $1/^{75}T_1T$ below T_C on the magnetic sites, which provides unambiguous evidence for the microscopic coexistence of bulk superconductivity and antiferromagnetic order. We measure a high value of $1/^{75}T_1T$ below T_N, which indicates that Ru doping induces itinerant electrons, and also a high density of low-energy excitations below T_c. These observations quantify the effects of Ru doping and provide extensive insight into the nature of the coexistence between superconductivity and magnetism.

Work at Renmin University of China was supported by the National Natural Science Foundation of China (Grants No. 11074304 and No. 11174365) and the National Basic Research Program of China (Grants No. 2010CB923004, No. 2011CBA00112 and No. 2012CB921704). Work at POSTECH was supported through the National Research Foundation of Korea by the Basic Research Program (Grants No. 2010-0005669 and No. 2012-013838) and by the Max Planck POSTECH/KOREA Research Initiative Program (Grant No. 2011-0031558).

Note added in proof.—Recently, we learned of an independent NMR study reporting the microscopic coexistence of AFM and SC in the underdoped iron superconductor $Ba_{1-x}K_xFe_2As_2$ [38].

*wqyu_phy@ruc.edu.cn

[1] C. de la Cruz *et al.*, Nature (London) **453**, 899 (2008).
[2] E. Wiesenmayer, H. Luetkens, G. Pascua, R. Khasanov, A. Amato, H. Potts, B. Banusch, H.-H. Klauss, and D. Johrendt, Phys. Rev. Lett. **107**, 237001 (2011).
[3] D. K. Pratt *et al.*, Phys. Rev. Lett. **106**, 257001 (2011).
[4] Y. Laplace, J. Bobroff, F. Rullier-Albenque, D. Colson, and A. Forget, Phys. Rev. B **80**, 140501(R) (2009).
[5] P. Marsik *et al.*, Phys. Rev. Lett. **105**, 057001 (2010).
[6] S. Nandi *et al.*, Phys. Rev. Lett. **104**, 057006 (2010).
[7] T. Iye, Y. Nakai, S. Kitagawa, K. Ishida, S. Kasahara, T. Shibauchi, Y. Matsuda, and T. Terashima, J. Phys. Soc. Jpn. **81**, 033701 (2012).
[8] A. J. Drew *et al.*, Nature Mater. **8**, 310 (2009).
[9] W. Bao, Q.-Z. Huang, G.-F. Chen, M. A. Green, D.-M. Wang, J.-B. He, and Y.-M. Qiu, Chin. Phys. Lett. **28**, 086104 (2011).
[10] R. M. Fernandes and J. Schmalian, Phys. Rev. B **82**, 014521 (2010).
[11] S. Maiti, R. M. Fernandes, and A. V. Chubukov, Phys. Rev. B **85**, 144527 (2012).
[12] Y. Nakai, T. Iye, S. Kitagawa, K. Ishida, H. Ikeda, S. Kasahara, H. Shishido, T. Shibauchi, Y. Matsuda, and T. Terashima, Phys. Rev. Lett. **105**, 107003 (2010).
[13] A. Thaler, N. Ni, A. Kracher, J. Yan, S. Bud'ko, and P. Canfield, Phys. Rev. B **82**, 014534 (2010).
[14] R. S. Dhaka *et al.*, Phys. Rev. Lett. **107**, 267002 (2011).
[15] V. Brouet *et al.*, Phys. Rev. Lett. **105**, 087001 (2010).
[16] N. Xu *et al.*, Phys. Rev. B **86**, 064505 (2012).
[17] M. G. Kim *et al.*, Phys. Rev. B **83**, 054514 (2011).
[18] M. J. Eom, S. Na, C. Hoch, R. Kremer, and J. Kim, Phys. Rev. B **85**, 024536 (2012).
[19] C. Bernhard *et al.*, arXiv:1206.7085.
[20] M.-H. Julien, H. Mayaffre, M. Horvatić, C. Berthier, X. D. Zhang, W. Wu, G. F. Chen, N. L. Wang, and J. L. Luo, Europhys. Lett. **87**, 37001 (2009).
[21] For a recent review, see A. M. Zhang, K. Liu, J. He, D. Wang, G. Chen, B. Normand, and Q. Zhang, Phys. Rev. B **86**, 134502 (2012).
[22] L. Zhang and D. J. Singh, Phys. Rev. B **79**, 174530 (2009).
[23] X. Qiu *et al.*, Phys. Rev. X **2**, 011010 (2012).
[24] K. Kitagawa, N. Katayama, K. Ohgushi, M. Yoshida, and M. Takigawa, J. Phys. Soc. Jpn. **77**, 114 709 (2008).
[25] K. Kitagawa, Y. Mezaki, K. Matsubayashi, Y. Uwatoko, and M. Takigawa, J. Phys. Soc. Jpn. **80**, 033 705 (2011).
[26] T. Moriya and K. Ueda, Solid State Commun. **15**, 169 (1974).
[27] L. Ma, G. Ji, J. Dai, J. He, D. Wang, G. Chen, B. Normand, and W. Yu, Phys. Rev. B **84**, 220505(R) (2011).
[28] T. Dey, P. Khuntia, A. V. Mahajan, S. Sharma, and A. Bharathi, J. Phys. Condens. Matter **23**, 475701 (2011).
[29] Y. Nagai, N. Hayashi, N. Nakai, H. Nakamura, M. Okumura, and M. Machida, New J. Phys. **10**, 103026 (2008).
[30] F. L. Ning, K. Ahilan, T. Imai, A. S. Sefat, M. A. McGuire, B. C. Sales, D. Mandrus, P. Cheng, B. Shen, and H.-H. Wen, Phys. Rev. Lett. **104**, 037001 (2010).
[31] S. W. Zhang, L. Ma, Y. D. Hou, J. Zhang, T.-L. Xia, G. F. Chen, J. P. Hu, G. M. Luke, and W. Yu, Phys. Rev. B **81**, 012503 (2010).
[32] W. Yu, L. Ma, J. He, D. Wang, T.-L. Xia, G. Chen, and W. Bao, Phys. Rev. Lett. **106**, 197001 (2011).
[33] S.-H. Baek, H. Lee, S. Brown, N. Curro, E. Bauer, F. Ronning, T. Park, and J. Thompson, Phys. Rev. Lett. **102**, 227601 (2009).
[34] Z. Li, D. Sun, C. Lin, Y. Su, J. Hu, and G.-q. Zheng, Phys. Rev. B **83**, 140506 (2011).
[35] H.-J. Grafe *et al.*, Phys. Rev. Lett. **101**, 047003 (2008).
[36] Y. Bang, H.-Y. Choi, and H. Won, Phys. Rev. B **79**, 054529 (2009).
[37] Y. Zhang, Z. R. Ye, Q. Q. Ge, F. Chen, J. Jiang, M. Xu, B. P. Xie, and D. L. Feng, Nat. Phys. **8**, 371 (2012).
[38] Z. Li *et al.*, arXiv:1204.2434.